Travel Time Denoising in Ultrasound Tomography

O. Roy, C. Li, and N. Duric

Delphinus Medical Technologies,
46701 Commerce Center Drive,
Plymouth, MI 48170, USA

Karmanos Cancer Institute,
4100 John R,
Detroit, MI 48201, USA

ABSTRACT

Accurate time delay estimation is critical for a wide range of remote sensing applications. We propose a technique that exploits the redundancy between absolute and relative time delays in transducer arrays as a means to reduce the level of noise present in the measurements. We formalize the problem of interest and present two different strategies to solve it. The first strategy is optimal in the mean square sense but requires a quadratic programming solver. The second approach is based on a sub-optimal iterative denoising technique. The effectiveness of our approach is demonstrated in the context of travel time tomographic imaging using numerical and physical breast mimicking phantoms as well as patient data.

Keywords: breast imaging, iterative denoising, quadratic programming, travel time estimation, ultrasound tomography.

1. INTRODUCTION

Time delay estimation plays an important role in a large number of applications including source localization,[1] and array calibration.[2] In ultrasound travel time tomography, the speed of sound can be imaged from travel time data measured using a transducer array surrounding the propagation medium of interest.[3,4] When this technique is applied to breast imaging, the sound speed image provides valuable information to detect cancer in tissues at an early stage.[5,6] In this case, accurate travel time estimation is critical in providing images that are free of artifacts and that display the correct sound speed values. To this end, a large number of travel time estimation methods have been designed over the last decades. Some of these methods are deterministic and exploit a large portion of the input signals, such as cross-correlation-based techniques (see, e.g., Refs. 7,8), while others are looking at local characteristics, such as the first break detector devised in Ref. 9. Some methods optimize statistical quantities such as the entropy.[10] For a review on existing methods, we refer the interested reader to the exposition in Ref. 11. Despite the tremendous research effort, accurate travel time estimation remains a challenging task in practice. Cross-talk among nearby transducers, non-ideal frequency response of piezoelectric sensors, and strong attenuation in the propagation medium are some of the reasons why the signals under observation are distorted, making the travel time estimation process difficult. In these scenarios, better accuracy can be obtained by explicitly taking into account the characteristics of the acquisition device. Another approach is to increase resilience to noise by means of data redundancy. In this paper, we adopt the later approach by combining two different travel time data sets measured using existing estimation techniques.

In a homogeneous medium, travel times are highly redundant. In fact, given the positions of the transducers, the travel times depend solely on a single parameter, namely the propagation sound speed. This redundancy is useful, for example, for calibration purpose.[2] In an inhomogeneous medium, however, such redundancy is

Further author information: (Send correspondence to O. Roy)
O. Roy - email: oroy@delphinusmt.com
C. Li - email: cli@delphinusmt.com
N. Duric - email: nduric@delphinusmt.com

Medical Imaging 2012: Ultrasonic Imaging, Tomography, and Therapy, edited by Johan G. Bosch,
Marvin M. Doyley, Proc. of SPIE Vol. 8320, 832006 · © 2012 SPIE
CCC code: 1605-7422/12/$18 · doi: 10.1117/12.911919

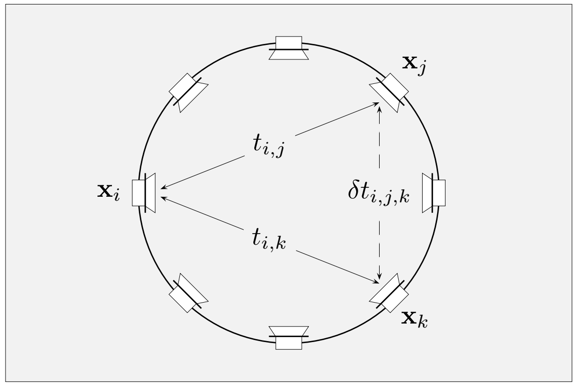

Figure 1. Tomographic setup with absolute and relative travel time measurements.

generally not apparent. Therefore, in addition to this set of *absolute* travel times (measured between an emitter and a receiver), we consider a set of *relative* travel times (measured between two receivers for a fixed emitter). The estimation methods for these two types of measurements are usually quite different. Absolute travel times may be computed using a first break detector,[9] while relative travel times can be computed using a cross-correlation method.[4,7] Our goal is to denoise these measurements jointly as a means to compute travel time estimates with improved accuracy. The rational behind our approach is to combine the strengths of absolute and relative travel time estimation techniques.

The outline of the paper is as follows. In Section 2, we formalize the denoising problem as a mean square minimization. We then present two methods to solve it. The first one resorts to a quadratic programming solver to find the optimal solution. In scenarios where the complexity of a quadratic solver cannot be afforded, we propose a second sub-optimal iterative denoising technique that builds upon the characteristic of relative travel time measurements. We also provide an analytical characterization of the optimal solution which can be used as the basis for a heuristic approach to travel time denoising. In Section 3, we demonstrate the effectiveness of our approach using noisy absolute and relative travel times measurements obtained from numerical and physical breast mimicking phantoms as well as patient data. Conclusions are given in Section 4.

2. TRAVEL TIME DENOISING

2.1 Problem Statement

Consider the tomographic setup depicted in Figure 1. It consists of n ultrasound transducers with positions $\mathbf{x}_i$ ($i = 0, 1, \ldots, n-1$). We denote by $t_{i,j}$ the absolute travel time measured between transducers i and j, and by $\delta t_{i,j,k}$, the relative travel time between transducers j and k when a signal is emitted from transducer i. For a given emitter i, we stack all absolute travel times into a vector $\mathbf{t}_i$, such that $(\mathbf{t}_i)_j = t_{i,j}$. We also form the relative travel time matrix $\mathbf{\Delta T}_i$ such that $(\mathbf{\Delta T}_i)_{j,k} = \delta t_{i,j,k}$. It holds that

$$\mathbf{\Delta T}_i = \mathbf{t}_i \mathbf{1}^T - \mathbf{1}\mathbf{t}_i^T \tag{1}$$

for $i = 0, 1, \ldots, n-1$. In the above equation, the vector $\mathbf{1}$ denotes the all-one vector of size n. In the presence of noise, however, the above equality does not hold anymore. Therefore, we would like to find the travel times that solve the following optimization problem

$$\min_{\substack{t_{i,j} \geqslant 0, j \neq i \\ t_{i,i}=0}} \left\| \mathbf{t}_i \mathbf{1}^T - \mathbf{1}\mathbf{t}_i^T - \hat{\mathbf{\Delta T}}_i \right\|^2 , \tag{2}$$

where $\hat{\mathbf{\Delta T}}_i$ denotes the noisy relative travel time measurements for emitter i. In the above minimization, we enforce the equality constraint $t_{i,i} = 0$ to prevent the system from having an infinite number of solutions. In this case, an absolute travel time is equivalent to a relative travel time where the emitter and the second receiver are the same ($t_{i,j} = \delta_{i,j,i}$). Note that, if reciprocity holds ($t_{i,j} = t_{j,i}$), the travel times for different emitters can be optimized jointly using a similar formulation. The cost function in the above minimization problem can be rewritten as

$$\begin{aligned}\left\|\mathbf{t}_i\mathbf{1}^T - \mathbf{1}\mathbf{t}_i^T - \hat{\mathbf{\Delta T}}_i\right\|^2 &= \left\|\mathbf{vec}\left(\mathbf{t}_i\mathbf{1}^T - \mathbf{1}\mathbf{t}_i^T - \hat{\mathbf{\Delta T}}_i\right)\right\|^2 \\ &= \left\|\mathbf{A}\mathbf{t}_i - \mathbf{b}_i\right\|^2 ,\end{aligned}$$

where

$$\mathbf{A} = \begin{bmatrix}\mathbf{0} & \mathbf{C}_1^T & \cdots & \mathbf{C}_{n-1}^T\end{bmatrix}^T \quad \text{and} \quad \mathbf{b}_i = \mathbf{vec}\left(\hat{\mathbf{\Delta T}}_i\right) .$$

In the above equations, **vec** denotes the vec operator where the elements in the matrix are scanned circularly along the diagonals, starting with the main diagonal. The matrix $\mathbf{0}$ is the all-zero matrix of size $n \times n$, and $\mathbf{C}_i$ the circulant matrix of size $n \times n$ whose first row has a one at indices 1 and i+1, and zero elsewhere. The minimization (2) can thus be written as

$$\min_{\substack{t_{i,j} \geqslant 0, j \neq i \\ t_{i,i}=0}} \mathbf{t}_i\, \mathbf{A}^T \mathbf{A}\, \mathbf{t}_i - 2\, \mathbf{b}^T \mathbf{A}\mathbf{t}_i . \tag{3}$$

2.2 Proposed Methods

We now present two methods to solve the problem stated above. The first one is based on the observation that the cost function (3) is of convex quadratic form. A wide range of quadratic programming solvers can be used to find the optimal solution. In particular, the popular MATLAB software provides the function `quadprog`. The following proposition provides an analytical characterization of this solution.

PROPOSITION 1. *Let* $\mathbf{C}$ *be the circulant matrix of size* $n \times n$ *with first row* $(n-1, -1, \ldots, -1)$*, and* $\mathbf{w}_i$ *the vector defined as* $\mathbf{w}_i = \bar{\mathbf{\Delta T}}_i\, \mathbf{1}$ *with*

$$\bar{\mathbf{\Delta T}}_i = \frac{1}{2}\left(\hat{\mathbf{\Delta T}}_i - \hat{\mathbf{\Delta T}}_i^T\right) .$$

We define $\mathcal{V}$ *as the set of vectors* $\mathbf{v}$ *of the form* $\mathbf{v} = \bar{\mathbf{C}}^\dagger\, \mathbf{w}_i$*, where* $\bar{\mathbf{C}}$ *contains a subset of the columns of the matrix* $\mathbf{C}$ *with indices* $j \neq i$*. The (unique) solution of the minimization* (3) *belongs to* $\mathcal{V}$*.*

Proof. See Appendix A. □

The above proposition is generally not of practical interest since it only provides with a large set of candidate solutions obtained by selecting the inequality constraints active at the optimum. However, in the scenario where quadratic programming solvers cannot be used (e.g., real-time applications), a heuristic approach is to solve (3) without the inequality constraints, and then to force the negative elements of the solution to zero. In this case, a strategy equivalent to that in Proposition 1 is to retain all the columns of the matrix $\mathbf{C}$, multiply its pseudo-inverse by the vector $\mathbf{w}_i$, and subtract the value $t_{i,i}$ to the result. Finally, the negative values can be set to zero. The advantage of this approach is that the pseudo-inverse can be implemented efficiently using fast Fourier transforms.

The second approach that we propose does not require quadratic programming solvers but generally provides with a sub-optimal solution. It is based on the following proposition.

PROPOSITION 2. *The relative travel time matrix* (1) *satisfies the following properties.*

1. *It is antisymmetric, that is,* $\mathbf{\Delta T}_i = -\mathbf{\Delta T}_i^T$.
2. *It has zero diagonal elements.*
3. *It is of rank at most 2.*

Algorithm 1 Relative Travel Time Matrix Denoising

Input: A noisy relative travel time matrix $\hat{\mathbf{\Delta T}}_i$.
Output: A cleaned relative travel time matrix $\mathbf{\Delta T}_i$.
Procedure:

1. Set $m = 0$ and $\hat{\mathbf{\Delta T}}_i^{(m)} = \varphi_1(\hat{\mathbf{\Delta T}}_i)$.
2. Compute $\hat{\mathbf{\Delta T}}_i^{(m+1)} = \varphi_3(\varphi_2(\hat{\mathbf{\Delta T}}_i^{(m)}))$.
3. If $\|\hat{\mathbf{\Delta T}}_i^{(m+1)} - \hat{\mathbf{\Delta T}}_i^{(m)}\| < \epsilon$ for some prescribed threshold ϵ, go to step 4. Otherwise, set $m \leftarrow m+1$ and go to step 2.
4. Output the matrix $\hat{\mathbf{\Delta T}}_i^{(m+1)}$.

Proof. The first two properties are trivial. The third one follows directly from the definition (1) since $\mathbf{rank}\left(\mathbf{t}_i\,\mathbf{1}^T - \mathbf{1}\,\mathbf{t}_i^T\right) \leqslant \mathbf{rank}\,\mathbf{t}_i\,\mathbf{1}^T + \mathbf{rank}\,\mathbf{1}\,\mathbf{t}_i^T \leqslant 2$. □

The third property suggests that, in the noiseless case, the entries of the matrix $\mathbf{\Delta T}_i$ are highly redundant. The intuition is that this redundancy can be used to denoise the travel time data. With noisy measurements, however, some of the above properties may not be satisfied. The idea is to successively enforce these properties as a means to denoise the travel time data. This is achieved by successively applying a number of mappings on the noisy matrix. The first mapping φ_1 enforces the antisymmetry of the matrix and is defined as $\varphi_1(\mathbf{\Delta T}_i) = (\mathbf{\Delta T}_i - \mathbf{\Delta T}_i^T)/2$. The second mapping φ_2 ensures that the matrix has zero diagonal elements by setting $(\varphi_2(\mathbf{\Delta T}_i))_{j,k} = (\mathbf{\Delta T}_i)_{j,k}$ if $j \neq k$, and zero otherwise. The third mapping implements the low rank condition by only retaining the two largest singular values. It is defined as $\varphi_3(\mathbf{\Delta T}_i) = \mathbf{U}_2\mathbf{\Lambda}_2\mathbf{V}_2^T$, that is, the best rank 2 approximation of $\mathbf{\Delta T}_i$ using its singular value decomposition. The proposed denoising procedure is summarized in Algorithm 1. It amounts to successively applying the above mappings on the original noisy data. Note that the antisymmetry condition imposed by the function φ_1 is not violated by any of the subsequent mappings. It thus only needs to be applied at the beginning of the algorithm. The convergence of this iterative procedure to a matrix that exhibits all of the three desired properties is supported by the following result.

PROPOSITION 3. *Any matrix sequence generated using Algorithm 1 contains a sub-sequence which converges to a matrix satisfying the three desired properties.*

Proof. The functions φ_2 is a continuous point-to-point mapping, and φ_3 is a closed point-to-set mapping (Theorem 2 of Ref. 12). Therefore, the composite point-to-set mapping $\varphi = \varphi_3\varphi_2$ used in Algorithm 1 is closed (Lemma 2 of Ref. 12). From Theorem 1 of Ref. 12, any sequence generated according to the update rule in step 2 of Algorithm 1 thus contains a subsequence that converges to a matrix satisfying the desired properties. □

It can be easily checked that the Frobenius norm of the relative travel time matrix is reduced at each iteration. This reduction quantifies the amount of noise that is removed by the method. At the end of the iterations, the de-noised absolute travel time vector $\hat{\mathbf{t}}_i$ can be read from the ith column of the denoised relative travel time matrix. A constraint of non-negativity can be applied subsequently. Unlike the previous approach, this iterative method is sub-optimal since there is no guarantee that the denoised relative travel time matrix produced by Algorithm 1 is closest in Frobenius norm to the original one.

2.3 Practical Considerations

In practice, it is generally not possible to measure all the entries of the relative travel time matrix. The reasons are manifold. First of all, the signals measured between some transducer pairs are too noisy to provide relevant absolute travel time estimates. This can happen, for example, if the incidence angle of the propagating wavefront is too large compared to the transducer beam width. The distortion incurred by a frequency dependent angular response also has an adverse effect on the estimation of the travel time. Moreover, the signal may be significantly attenuated by the propagation medium (e.g., in dense breast), preventing a reasonable estimate of the travel time.

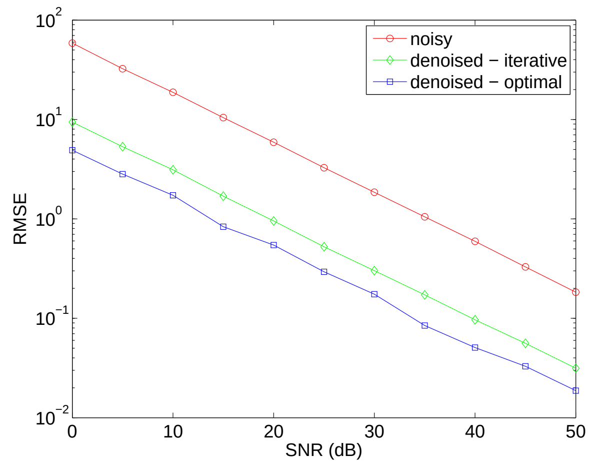

Figure 2. Travel time estimation error using the proposed algorithms.

Relative travel time estimation between two signals (e.g., using a cross-correlation method) becomes challenging when the signals have different shapes. The method thus works best for nearby transducers.

For the above reasons, the relative travel time matrix is generally incomplete. In this case, the quadratic solver can still be used by simply removing the entries that are not available. With the iterative approach, however, missing entries must be first interpolated. Low-rank matrix completion algorithms can be used for that purpose (see, e.g., Ref. 13). Since our matrix is very specific, custom interpolation techniques based on geometrical considerations can also be devised.

3. RESULTS

3.1 Numerical Phantom

To demonstrate the effectiveness of our approach in the context of ultrasound tomography, we have considered the numerical sound speed phantom shown in Figure 3(a). It is imaged by an array of $n = 64$ transducers. The data set has been generated using the time-domain waveform propagation scheme described in Ref. 14. Absolute travel times have been estimated using the method exposed in Ref. 9. Relative travel times have been computed from these absolute travel times, and additive white Gaussian noise has been added to meet a desired SNR.

In Figure 2, we plot the RMSE of the estimated travel times as a function of the SNR for the original noisy data, the data denoised using the iterative algorithm, and the data denoised using the mean-square optimal approach by means of a quadratic programming solver. We observe that significant noise reduction can be achieved using the proposed methods. The iterative technique, while being suboptimal, achieves most of the noise reduction. In this case, only a couple of iterations were needed. In Figure 3, we plot the sound speed images reconstructed from the three travel time data sets obtained with an SNR of 30 dB. We observe that the proposed denoising methods significantly improve the image quality. Moreover, we can clearly visualize the sub-optimality of the iterative scheme compared to the optimal quadratic programming method.

3.2 Physical Phantom and Patient Data

The synthetic results presented above demonstrate the potential of our approach in an ideal scenario. In practice, however, it is impossible to measure the entire set of relative travel time differences. In fact, only signals acquired by nearby transducers can be accurately compared by means of a cross-correlation method. The denoising power of the proposed method is thus greatly reduced. For these experiments, the data sets were acquired using the 256 transducer ring of the CURE prototype at the Karmanos Cancer Institute.[5] We have generated absolute travel times using the first break detector devised in Ref. 9. Relative travel times were generated using the simple cross-correlation method used in Ref. 4. For each receiver, we have considered an aperture composed of the four closest receivers (two on each side). In other words, our relative travel time matrix is a band diagonal matrix

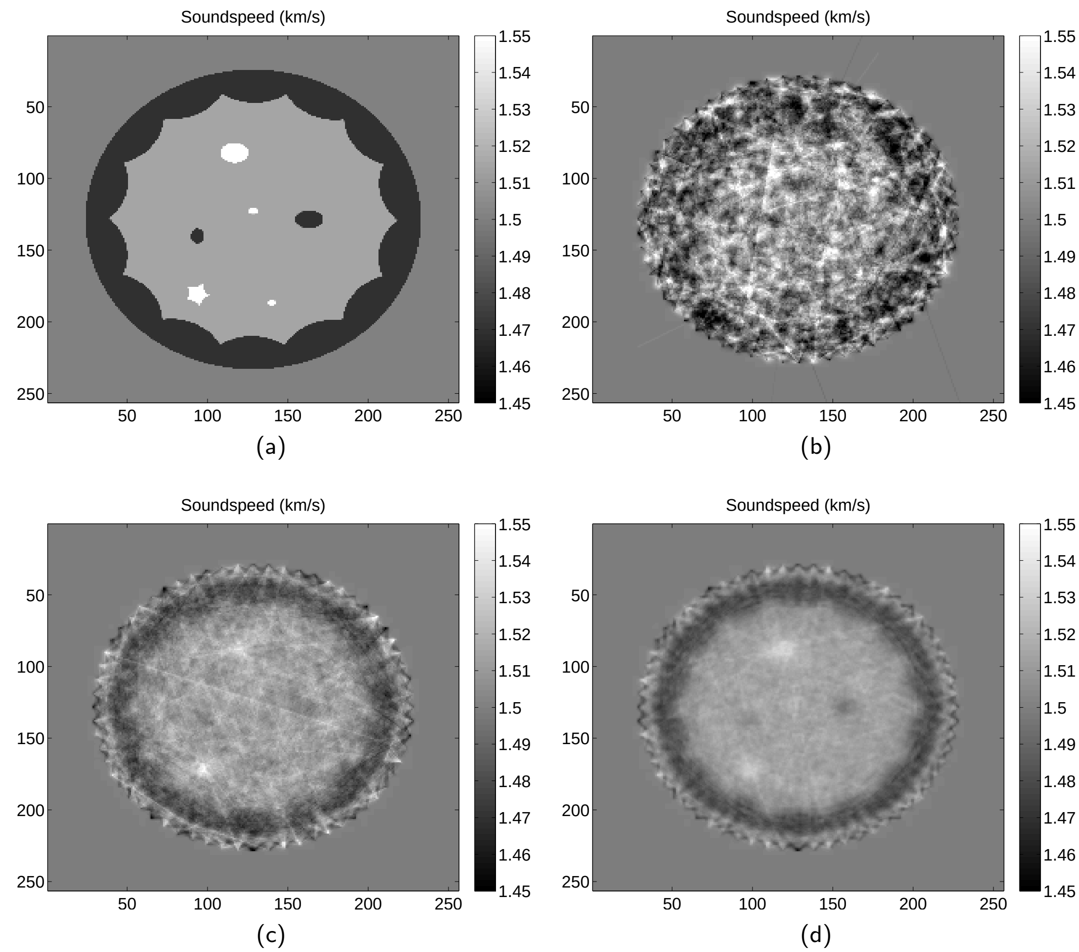

Figure 3. Sound speed reconstructions using travel time tomography. (a) Original sound speed image. Reconstruction using (b) the noisy data set, (c) the data set denoised using the iterative algorithm, and (d) the data set denoised using the optimal algorithm.

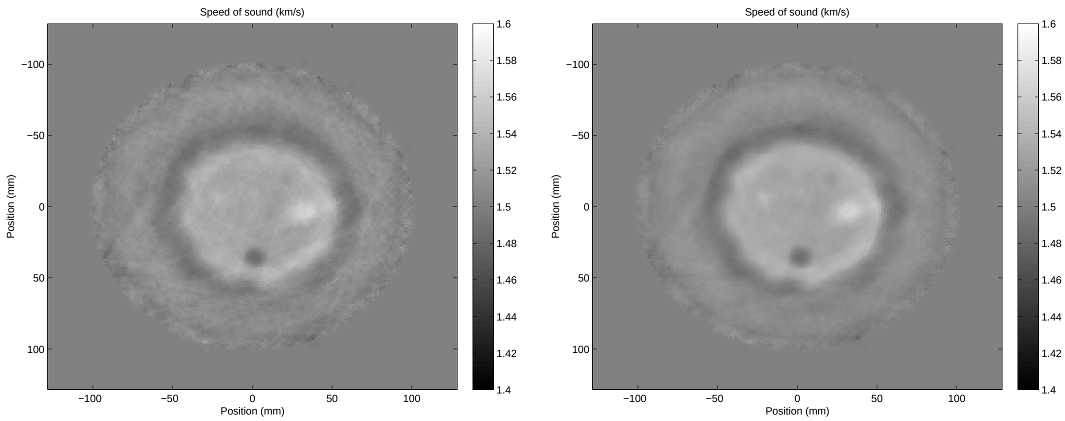

(a) (b)

Figure 4. Sound speed reconstruction of a breast mimicking phantom. (a) Reconstruction using the original data set. (b) Reconstruction using the denoised data set.

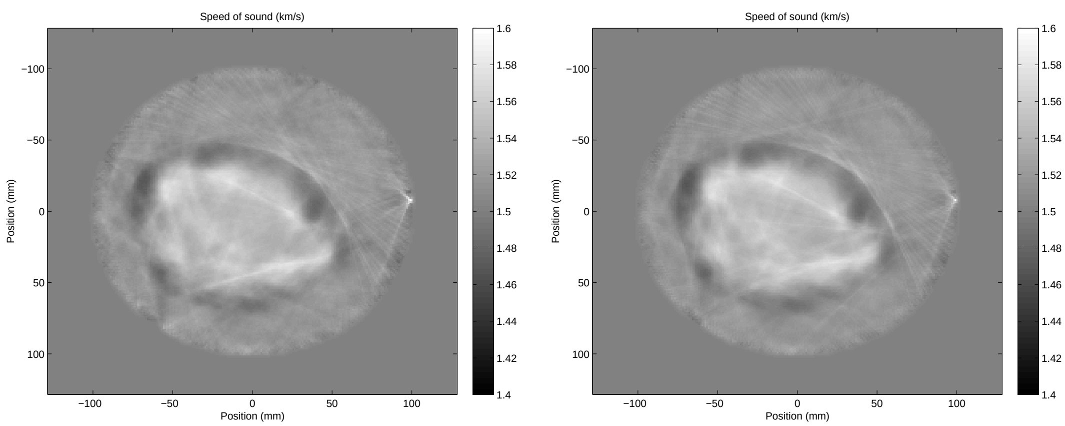

(a) (b)

Figure 5. Sound speed reconstruction of patient data. (a) Reconstruction using the original data set. (b) Reconstruction using the denoised data set.

with a band of width five. The quadratic programming method was used to denoise the absolute travel time measurements.

In Figure 4, we show the reconstruction results obtained for a physical breast mimicking phantom. We observe that the denoised image is generally smoother but provides a sharper rending of the boundaries of the subcutaneous fat layer. Absolute travel times along the rays delimiting these boundaries are usually difficult to estimate due to refraction effects. In this case, the information obtained by comparing neighboring signals provides good denoising capability. Due to the limited number of relative travel time measurements, the denoising power is however significantly smaller than the synthetic case presented above.

In Figure 5, we consider the reconstruction of a patient data set. In this scenario, the relative travel time estimates allow to reduce the artifacts that arise in the 7 o'clock region due to the lack of absolute travel time information. This information recovery can also be visualized on the absolute travel time matrices displayed in Figure 6. We clearly observe that a large number of the missing travel time measurements (set to 0) can be estimated using the proposed denoising method. A few ray artifacts arising in the same region are also reduced.

4. CONCLUSIONS

We have presented a novel denoising method that uses relative travel time estimates to denoise absolute travel time measurements. The effectiveness of our scheme has been demonstrated in the context of ultrasound tomog-

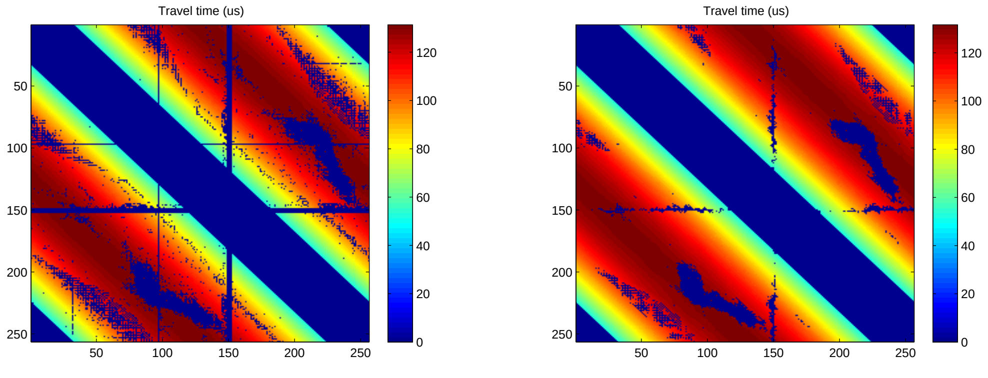

(a) (b)

Figure 6. Travel time denoising using patient data. (a) Original travel time matrix. (b) Denoised travel time matrix.

raphy using numerical and physical breast mimicking phantoms as well as patient data. We have shown that the denoising capability of the proposed scheme depends on the availability of a large set of relative travel time measurements computed between an aperture of nearby transducers. The cross correlation method used in this paper is fairly simple and works best for small apertures. Further research is needed to find relative travel time estimation techniques that allow for larger apertures in order to use the full potential of the proposed denoising scheme.

APPENDIX A. PROOF OF PROPOSITION 1

The cost function (2) can be expressed as

$$\begin{aligned}\left\|\mathbf{t}_i\mathbf{1}^T-\mathbf{1}\mathbf{t}_i^T-\boldsymbol{\Delta}\hat{\mathbf{T}}_i\right\|^2 &= 2n\left\|\mathbf{t}_i\right\|^2-2\,\mathbf{tr}\left(\mathbf{t}_i^T\mathbf{1}\,\mathbf{t}_i^T\mathbf{1}\right)+\mathbf{tr}\left(\boldsymbol{\Delta}\hat{\mathbf{T}}_i\,\boldsymbol{\Delta}\hat{\mathbf{T}}_i^T\right)-2\,\mathbf{tr}\left(\boldsymbol{\Delta}\hat{\mathbf{T}}_i\,\left(\mathbf{1}\mathbf{t}_i^T-\mathbf{t}_i\mathbf{1}^T\right)\right)\\ &= 2n\left\|\mathbf{t}_i\right\|^2-2\,\mathbf{tr}\left(\mathbf{t}_i^T\mathbf{1}\,\mathbf{t}_i^T\mathbf{1}\right)+\mathbf{tr}\left(\boldsymbol{\Delta}\hat{\mathbf{T}}_i\,\boldsymbol{\Delta}\hat{\mathbf{T}}_i^T\right)-4\,\mathbf{tr}\left(\boldsymbol{\Delta}\bar{\mathbf{T}}_i\,\mathbf{1}\mathbf{t}_i^T\right)\,,\end{aligned}$$

where in the second equality we use the fact that $\mathbf{tr}\left(\mathbf{A}\right)=\mathbf{tr}\left(\mathbf{A}^T\right)$ and $\mathbf{tr}\left(\mathbf{AB}\right)=\mathbf{tr}\left(\mathbf{BA}\right)$ for conforming matrices, and define

$$\boldsymbol{\Delta}\bar{\mathbf{T}}_i=\frac{1}{2}\left(\boldsymbol{\Delta}\hat{\mathbf{T}}_i-\boldsymbol{\Delta}\hat{\mathbf{T}}_i^T\right)\,.$$

Defining $\mathbf{w}_i=\boldsymbol{\Delta}\bar{\mathbf{T}}_i\,\mathbf{1}$, the minimization (2) can be rewritten as

$$\begin{aligned}\min_{\substack{t_{i,j}\geqslant 0, j\neq i\\ t_{i,i}=0}}\left\|\mathbf{t}_i\mathbf{1}^T-\mathbf{1}\mathbf{t}_i^T-\boldsymbol{\Delta}\hat{\mathbf{T}}_i\right\|^2 &= \min_{\substack{t_{i,j}\geqslant 0, j\neq i\\ t_{i,i}=0}}\;2n\left\|\mathbf{t}_i\right\|^2-2\,\left(\mathbf{t}_i^T\mathbf{1}\right)^2-4\,\mathbf{w}_i^T\mathbf{t}_i\\ &= \min_{\substack{t_{i,j}\geqslant 0, j\neq i\\ t_{i,i}=0}}\;n\sum_{j=0}^{n-1}t_j^2-\left(\sum_{j=0}^{n-1}t_j\right)^2-2\sum_{j=0}^{n-1}w_jt_j\,.\end{aligned}$$

Let us define $f(\mathbf{t}_i)$ as the above cost function, $g_j(\mathbf{t}_i)=-t_{i,j}\leqslant 0$ as the inequality constraints, and $h(\mathbf{t}_i)=t_{i,i}=0$ as the equality constraint. Since f and g_j are continuously differentiable, and h is affine, the Karush-Kuhn-Tucker conditions provide necessary and sufficient conditions for optimality. In particular, the stationarity condition

$$\nabla f(\hat{\mathbf{t}}_i)+\sum_{j\neq i}\mu_j\nabla g_j(\hat{\mathbf{t}}_i)+\lambda\nabla h(\hat{\mathbf{t}}_i)=0$$

implies that the multipliers μ_j must satisfy

$$\mu_j=2\left(n\,\hat{t}_{i,j}-\sum_{k=0}^{n-1}\hat{t}_{i,j}-w_{i,j}\right)\,.$$

The complementary slackness condition $\mu_j g_j(\mathbf{t}_i) = 0$ evaluates as

$$\left(n\,\hat{t}_{i,j} - \sum_{k=0}^{n-1} \hat{t}_{i,j} - w_{i,j} \right) \hat{t}_{i,j} = 0\,.$$

The solution $\hat{\mathbf{t}}$ thus satisfies

$$\mathbf{C}\,\hat{\mathbf{t}}_i = \mathbf{w}_i\,,$$

where $\mathbf{C}$ is the circulant matrix defined in Proposition 1. The above system of equations has an infinite number of solutions. When no inequality constraint is active at the optimum, the optimal solution can be found by removing column i of the matrix $\mathbf{C}$ and find the solution using its pseudo-inverse. When some inequality constraints are active at the optimum, the corresponding columns must also be removed. In general, the optimal solution belongs to the set of vectors $\mathcal{V}$ defined in Proposition 1.

REFERENCES

1. J. Chen, Y. Kung, and R. Hudson, "Source localization and beamforming," *IEEE Signal Processing Magazine* **19**, pp. 30–39, Mar. 2002.
2. O. Roy, I. Jovanovic, N. Duric, L. Poulo, and M. Vetterli, "Robust array calibration using time delays with application to ultrasound tompography," in *SPIE Medical Imaging*, **7968**, Mar. 2011.
3. A. Hormati, I. Jovanovic, O. Roy, and M. Vetterli, "Robust ultrasound travel-time tomography using the bent ray model," in *SPIE Medical Imaging*, **7929**, Mar. 2010.
4. C. Li, N. Duric, O. Rama, A. Burger, L. Polin, and N. Nechiporchik, "Double difference tomography for breast ultrasound sound speed imaging," in *SPIE Medical Imaging*, **7968**, Mar. 2011.
5. N. Duric, P. Littrup, L. Poulo, and A. Babkin, "Detection of breast cancer with ultrasound tomography: First results with the Computed Ultrasound Risk Evaluation (CURE) prototype.," *Medical Physics* **34**, pp. 773–785, Feb. 2007.
6. R. G. Pratt, L. Huang, N. Duric, and P. Littrup, "Sound-speed and attenuation imaging of breast tissue using waveform tomography of transmission ultrasound data," in *SPIE Medical Imaging*, **6510**, Mar. 2007.
7. C. H. Knapp and G. C. Carter, "The generalized correlation method for estimation of time delay," *IEEE Transactions on Acoustics, Speech and Signal Processing* **ASSP-24**, pp. 320–327, Apr. 1976.
8. J. Benesty, J. Chen, and Y. Huang, "Time-delay estimation via linear interpolation and cross correlation," *IEEE Transactions on Speech and Audio Processing* **12**, pp. 509–519, Sept. 2002.
9. C. Li, L. Huang, N. Duric, H. Zhang, and C. Rowe, "An improved automatic time-of-flight picker for medical ultrasound tomography," *Ultrasonics* **49**, pp. 61–72, Jan. 2009.
10. J. Benesty, Y. Huang, and J. Chen, "Time delay estimation via minimum entropy," *IEEE Signal Processing Letters* **14**, pp. 157–160, Mar. 2007.
11. J. Chen, J. Benesty, and Y. Huang, "Time delay estimation in room acoustic environments: an overview," *EURASIP Journal on Applied Signal Processing* **2007**, pp. 1–19, Jan. 2006.
12. J. A. Cadzow, "Signal enhancement – A composite property mapping algorithm," *IEEE Transactions on Acoustics, Speech and Signal Processing* **36**, pp. 49–62, Jan. 1988.
13. R. Keshavan, A. Montanari, and S. Oh, "Matrix completion from a few entries," *IEEE Transactions on Information Theory* **56**, pp. 2980–2998, June 2010.
14. O. Roy, I. Jovanovic, A. Hormati, R. Parhizkar, and M. Vetterli, "Sound speed estimation using wave-based ultrasound tomography: Theory and GPU implementation," in *SPIE Medical Imaging*, **7629**, Mar. 2010.